Environmental Science
Nano

www.rsc.org/es-nano

Volume 1 | Number 1 | Jan 2013 | Pages 1–100

ROYAL SOCIETY OF CHEMISTRY

ROYAL SOCIETY
OF CHEMISTRY

rsc.li/es-nano

Optimized protocols for the small-scale synthesis of isotopically labeled silver nanoparticles and an evaluation of their environmental tracing capabilities.

Nano Impact Statement

The application of isotopically labeled nanoparticles enables the accurate and precise tracing of these materials in exposure experiments, even when carried out at low and environmentally relevant concentrations. However, isotopically labeled nanoparticles are not commercially available and published synthesis techniques tend to be unsuitable for use with an isotopically enriched pre-cursor material. This is the first study to provide protocols specifically optimized for the small-scale, high yield synthesis of isotopically labeled silver nanoparticles with defined sizes. The synthesis techniques are rigorously assessed and shown to be fit for purpose. Apart from their isotope composition the silver nanoparticles produced using both a 'natural' and an isotopically enriched precursor are shown to be indistinguishable. In addition the nanoparticle suspensions are shown to be stable after 12 months storage. A comprehensive evaluation of the nanoparticles produced here demonstrates the detection capabilities possible when these materials are employed in environmental tracer studies. Detailed equations are also presented to show how the quantification of an enriched isotope label can be achieved from the isotope ratio of a sample.

1 # Synthesis and characterization of isotopically labeled silver

2 # nanoparticles for tracing studies

3

4

5 Adam Laycock[1,2,*], Björn Stolpe[3], Isabella Römer[3], Agnieszka Dybowska[2], Eugenia Valsami-Jones[3,2],

6 Jamie R. Lead[3,4], Mark Rehkämper[1,2]

7 [1] Department of Earth Science & Engineering, Imperial College London, South Kensington, London SW7 2AZ,

8 England

9 [2] Department of Earth Sciences, Natural History Museum, Cromwell Road, London SW7 5BD, England

10 [3] School of Geography, Earth and Environmental Sciences, University of Birmingham, Edgbaston, Birmingham, B15

11 2TT, England

12 [4] Center for Environmental Nanoscience and Risk, Department of Environmental Health Sciences, Arnold School of

13 Public Health, University of South Carolina, Columbia, SC 29208, USA

14
15
16
17
18
19
20
21
22
23
24
25
26
27
28
29
30
31
32
33
34
35
36
37

38 *Corresponding author: a.laycock10@imperial.ac.uk
39   +44 20 7594 7140
40

1 **Abstract**

2 Silver nanoparticles (AgNPs) are ever more being used in industrial processes and consumer products,

3 resulting in increasing emissions to the natural environment. To understand the behavior and

4 environmental fate of AgNPs, it is paramount that they can be traced in complex natural samples from

5 exposures at high sensitivity. The technique of stable isotope labeling is ideally suited for this purpose.

6 To support such applications, we present a detailed evaluation of techniques for the preparation of stable

7 isotope labeled AgNPs and demonstrate that isotopically modified particles are only distinguishable from

8 particles with a natural isotope composition by their strong isotopic signature. Monodisperse suspensions

9 of citrate-stabilized AgNPs with target sizes sizes of 17, 20 and 30 nm were synthesized by reduction of

10 silver nitrate solutions with sodium borohydride. The AgNP suspensions were produced using both

11 natural Ag, which is comprised of the two stable isotopes ^{107}Ag (52%) and ^{109}Ag (48%), and Ag enriched

12 to 99.2% in ^{107}Ag. Synthesis was reliably reproduced on three separate occasions in two laboratories.

13 The AgNPs were characterized using dynamic light scattering (DLS) shortly after synthesis and after up

14 to 12 months storage. Some of the batches were also characterized using transmission electron

15 microscopy (TEM) and asymmetric flow field-flow fractionation (FlFFF). The particle size distributions

16 showed good reproducibility between the laboratories and stability over 12 months of storage.

17 Importantly, the ^{107}Ag-enriched particles were indistinguishable in size and shape from particles with a

18 natural isotope composition. The reliability, control on particle size, and high yield of about 80%,

19 demonstrate that the synthesis technique is well suited for small-scale production of isotopically labeled

20 AgNPs. Isotope mass balance calculations furthermore show that the application of labeling enables

21 tracing sensitivities for AgNPs that are at least 40 times, and possibly up to 4000 times, higher than

22 those achievable with bulk Ag concentration measurements and experiments with exposure

23 concentrations that approach predicted environmental levels are possible, if the most precise isotopic

24 measurement techniques are employed.

25

27

1   **1. Introduction**

2   As a consequence of the ubiquitous use of Ag in the photography and imaging industries, anthropogenic

3   emissions of Ag and their environmental fate have been monitored for many decades [1]. Whilst the rise of

4   digital photography has significantly reduced such emissions, new concerns have arisen as engineered

5   Ag nanoparticles (AgNPs) are increasingly employed in a broad range of industrial processes and

6   consumer products and emitted into the environment [1, 2]. Whilst not comprehensive, there are currently

7   390 products (November 2013) listed on the Woodrow Wilson Database[3] that incorporate nano-silver,

8   demonstrating the diverse range of products in which this nanomaterial is found. A focus of current

9   research and debate is whether there are (nano-) specific effects, which increase the bioavailability and

10   toxicity of Ag when present in nanoparticulate form [2]. This concern has prompted numerous studies to

11   investigate the environmental transport, behavior, fate and ecotoxicology of engineered AgNPs.

12   Ideally, such studies are carried out at 'realistic' environmental conditions, whereby exposures employ

13   NM (nanomaterial) concentrations that are similar to or not far removed from present or predicted values.

14   Recently, Gottschalk, et al. [4] compiled and reviewed measured and modeled environmental

15   concentrations of engineered NMs. Based on the reviewed data, predicted environmental levels of

16   engineered nano-Ag are in the range of 0.1 to 100 ng L^{-1} for surface waters, 1 to 100 ng L^{-1} for effluents

17   of waste water treatment plants, 1 to 1000 µg kg^{-1} for biosolids, 1 to 10 µg kg^{-1} for sediments, and 0.1 to

18   1000 µg kg^{-1} for soils. Significantly, these levels are roughly similar to the natural Ag background

19   concentrations of these materials [5].

20   Studies that interrogate the environmental fate of AgNPs typically employ concentration measurements

21   by ICP-MS to quantify the presence of Ag (from NPs) in exposure systems. Such analyses are

22   straightforward but require that exposures employ AgNP concentrations that exceed 'realistic'

23   environmental levels by several orders of magnitude. This requirement follows from (i) the comparatively

24   high natural Ag background (see above), and (ii) the condition that unequivocal tracing of AgNPs relies

25   on the detection of anomalies in Ag concentration that clearly exceed these background levels. For

26   example, Shoults-Wilson, et al. [6] used AgNP concentrations of 10 to 1000 mg kg^{-1} in soil exposures of

27   the earthworm *Eisenia fetida*, whilst Zhao and Wang [7] applied AgNPs at 20 to 500 µg L^{-1} in a waterborne

28   exposure of *Daphnia magna*. It is conceivable that ecotoxicity studies, which are carried out at such high

29   (and unrealistic) AgNP concentrations, may induce and thus identify distinct patterns of particle behavior

30   and biological interactions that are only relevant for the high particle concentrations that are employed.

31   The challenge is, therefore, to investigate whether the same effects are also observed at low but

32   environmentally relevant NP levels.

33   To circumvent the limited sensitivity of concentration tracing, alternative NM tracing methods have been

34   explored, particularly fluorescent coatings [8, 9] and radiolabelling [10-12], but both techniques have

35   associated drawbacks. The application of fluorescent coatings can affect the surface chemistry of the

36   materials and influence their behavior, such as changes to and suppression of dissolution [13]. The

37   coatings may furthermore dissociate from the NPs [14] and free ions from NP dissolution cannot be traced

38   with this method. Radiolabelled nanomaterials are produced by activation in a nuclear reactor [15, 16] and

1   the technique is therefore hindered, as specialist equipment, dedicated laboratories and licenses are

2   required for the handling of radioactive materials. A further disadvantage is the often short half-lives of

3   the radiolabels.

4   An attractive alternative method of labeling, which does not suffer from the above drawbacks, involves

5   the application of enriched stable isotopes. The basic approach of stable isotope labeling relies on the

6   detection of changes in a diagnostic isotope ratio, which are produced in an experimental system by the

7   introduction of a 'contaminant' that is prepared from a highly enriched single isotope of the target

8   element. In the case of Ag, the natural form of the element consists of nearly equal amounts of the

9   isotopes ^{107}Ag and ^{109}Ag but highly enriched (to >99%) ^{107}Ag can be purchased from a number of

10 sources. The introduction of essentially pure ^{107}Ag into an exposure will not only increase the total Ag

11 concentration of the system but also change the ^{107}Ag/^{109}Ag isotope ratio, such that this exceeds the

12 natural value of ~1. The magnitude of the isotopic perturbation hereby depends on the relative

13 contributions of enriched ^{107}Ag to natural Ag (Fig. 1). As (i) natural variations in isotope compositions are

14 typically small for most elements and (ii) isotope ratios can be measured much more precisely than

15 absolute concentrations, the use of enriched stable isotopes provides an extremely selective and

16 sensitive means of elemental tracing, even in the presence of high natural background levels [17, 18].

17 Consequently, the stable isotope approach has been used successfully for several decades in the fields

18 of medical, life and environmental sciences, when highly sensitive and precise tracing methods were

19 required [19, 20].

20 More recently, it has been shown that stable isotope tracing can also be applied to nanomaterials, with

21 pioneering studies of ZnO and CuO NPs [17, 18, 21-23]. A unique requirement of such investigations is that

22 the labeled NPs must be specifically prepared, from a single, highly enriched stable isotope form of the

23 element. Particular advantages of this approach are (i) high versatility, as it can, in principle, be applied

24 to any NP with a multi-isotopic element as main constituent; (ii) the label cannot be lost by dissociation or

25 degradation; and (iii) the unique isotopic signature of the element remains traceable even if the

26 speciation of the original material changes, for example by dissolution. The methodology, however, also

27 requires that a suitable protocol for the preparation of labeled NPs is available. Whilst recipes for the

28 synthesis of various NMs with defined sizes and properties are abundant in the literature, most of these

29 methods are either unsuitable for the synthesis of stable isotope labeled NPs or they provide insufficient

30 documentation for this purpose. This conclusion follows from the relatively high price of commercially

31 available enriched stable isotopes, which typically cost about $2 to $20 per mg of metal or metal oxide.

32 Given this non-negligible cost, methods for the preparation of isotopically labeled NMs must be optimized

33 with a focus on small-scale synthesis, reliability and high yields. These factors, however, are generally

34 not considered in conventional synthesis protocols, where particle size and shape are typically of higher

35 priority.

36 In this study, we have examined existing protocols to develop techniques for the optimized preparation of

37 isotopically labeled AgNPs with distinct sizes. Rigorous evaluations demonstrate that the methods are

38 suitable for routine and reliable small-scale synthesis of stable isotope labeled AgNPs at yields of ~80%.

39 The characterization of both labeled AgNPs and control samples produced from natural Ag furthermore

1   unequivocally establishes that the labeling process does not generate distinct or unusual physico-

2   chemical particle properties. This is essential in order to demonstrate that isotopically modified AgNPs

3   are equivalent to AgNPs with a natural isotope composition and to validate the findings of any studies

4   carried out using isotopically modified AgNPs, such as the recent investigation of Gigault and Hackley [24].

5   These workers[24] used asymmetric-flow field flow fractionation system coupled with on-line ICP-MS

6   detection to show how a stable isotope label may be used to confirm the presence of Ag from an

7   isotopically enriched source within a natural sample. While this technique offers rapid and definitive

8   results it does not allow accurate quantification of the enriched material in a sample. Our study assesses

9   the utility of the isotope tracing approach beyond the level of simply detecting the isotope label in a

10   sample. To this end, we present the results of simple model calculations, which reveal the lowest levels

11   at which isotopically labeled AgNPs can be detected and accurately quantified in relevant natural

12   samples by stable isotope tracing, when different common mass spectrometric methods are employed

13   for analysis.

14   **2. Experimental**

15   The AgNPs were synthesized by appropriately modified standard reduction methods [25, 26]. In particular,

16   batches of particles with 3 target sizes were produced from both natural Ag and enriched ^{107}Ag. Two

17   operators carried out the AgNP synthesis on three occasions in two laboratories and the reproducibility

18   of the methods was assessed by comprehensive characterization of all NP batches produced.

19   *2.1 Choice of isotope label*

20   When selecting an enriched stable isotope for labeling there are several key considerations, including

21   degree of isotopic enrichment, cost of the material and the diagnostic isotope ratio that will be monitored

22   for the purpose of tracing. A detailed discussion of these factors is provided by Larner and Rehkämper [27].

23   Silver has two naturally occurring stable isotopes, ^{107}Ag and ^{109}Ag, that have near equal natural

24   abundances of 51.8% and 48.2%, respectively, and both are available at an enrichment of about 99%

25   (Isoflex U.S.A., February 2012). As both isotopes are equally suitable for tracing, ^{107}Ag was chosen here

26   for labeling because it was marginally cheaper than ^{109}Ag (Isoflex U.S.A., February 2012).

27   *2.2 Chemicals and reagents*

28   Powdered Ag metal enriched to 99.2% in ^{107}Ag (Isoflex U.S.A.) was converted to ^{107}AgNO$_3$ by dissolution

29   in 15.4 M HNO$_3$ and subsequent evaporation to dryness. Natural AgNO$_3$ (>99% purity), trisodium citrate

30   dihydrate (>99% purity) and sodium borohydride (99.99% trace metals basis) were purchased from

31   Sigma-Aldrich. Water of >18.2 MΩ cm quality (Millipore, UK) and quartz-distilled mineral acids were used

32   throughout. Dilute artificial seawater (dilute-ASW) with a salinity of about 16 PSU was produced by

33   dissolution of 32 g of Tropic Marine Salt in 2 L purified water and used as medium for a dialysis study to

34   assess dissolution.

35

36

1   *2.3 Synthesis*

2   The synthesis protocols used here were adapted from the methods outlined by Römer, et al. [26]. Three

3   protocols, denoted AgNP1, AgNP2, and AgNP3 (Table 1), were applied to produce particles with target

4   sizes of 30, 20 and 17 nm, both with enriched ^{107}Ag (denoted as 107-AgNP1, 107-AgNP2 and 107-

5   AgNP3, respectively) and natural Ag (denoted as Nat-AgNP1, Nat-AgNP2 and Nat-AgNP3). The NP

6   batches are further designated to indicate (i) the date of synthesis, either May or October 2012 (May12

7   or Oct12), and (ii) the laboratory in which synthesis was conducted, either at the Facility for

8   Environmental Nanoscience Analysis and Characterization (FENAC) at the University of Birmingham or

9   the MAGIC (Mass Spectrometry and Isotope Geochemistry at Imperial College) Laboratories at Imperial

10   College London, (F and IC respectively). For example, the non-labeled AgNPs with a 20 nm target size

11   prepared at FENAC in October 2012 are identified as Nat-AgNP2-Oct12-F (Table 1).

12   For synthesis, 100 mL aqueous solutions of 0.25 mM sodium citrate and 0.30 mM silver nitrate were

13   cooled to 4°C, combined in a conical flask and vigorously stirred. To the AgNP1 and AgNP2 batches, 6

14   mL aqueous $NaBH_4$ was added at a concentration of 10 and 1 mM, respectively, whilst nothing was

15   added to the AgNP3 batch at this stage. For all protocols, the mixtures were then boiled for 90 minutes,

16   after which the AgNP1 and AgNP2 mixtures were removed from the heat. For the AgNP3 batches, 6 mL

17   of 10 mM aqueous $NaBH_4$ solution were added to the mixture after 90 minutes of boiling, followed by

18   boiling for a further 10 minutes. All solutions were thereafter allowed to cool overnight in the dark at room

19   temperature. A summary of the synthesis protocols is given in Table 2.

20   The particle suspensions were filtered through 0.1 µm pore-size cellulose acetate filters to remove any

21   larger (non-nano) particulates. Non-reacted reagents were thereafter removed by either diafiltration or

22   dialysis. In the diafiltration method, the volume of the suspensions was reduced to ~20 mL without drying,

23   by forcing through a 1 kDa (~1 nm) molecular weight cut-off (MWCO) regenerated cellulose ultrafiltration

24   membrane (Amicon, Millipore) using a nitrogen gas pressurized and stirred filtration cell. The suspension

25   volume was then re-adjusted back to ~200 mL using 0.15 mM sodium citrate solution and this process

26   was repeated three times. For the dialysis method, the suspensions were transferred to 1 kDa MWCO

27   dialysis bags (Spectra/Por) followed by dialysis against 5 L of 0.15 mM sodium citrate solution for 72

28   hours. The AgNP suspensions in aqueous Na-citrate from all protocols and filtration methods were

29   thereafter stored in the dark at 4°C.

30   2.4 *Characterization of particle size*

31   *2.4.1 Dynamic light scattering (DLS)*

32   The hydrodynamic diameter (average size) and polydispersity index (PDI) of the AgNPs were

33   determined at 25°C using a Zetasizer Nano ZS ZEN3600 (Malvern Instruments Ltd. Malvern, UK)

34   operating with a He-Ne laser at a wavelength of 633 nm and measuring back-scattered light at 173°

35   relative to the incident beam. Each sample was analyzed at least 5 consecutive times within 24 hours of

36   filtering. Some samples were analyzed after up to 12 months storage to give an indication of particle

37   stability.

1   *2.4.2 Transmission electron microscopy (TEM)*

2   For TEM analyses, the AgNPs from 10 mL of the stock suspensions were deposited onto 300 mesh

3   Formvar/carbon coated Cu-grids by ultracentrifugation (Beckman L-75) at 30,000 rpm for 60 minutes.

4   Grids were then rinsed by immersing in 18 MΩ water for a few seconds and dried overnight. The TEM

5   micrographs were obtained from 3 to 5 different areas on each grid, at a magnification of 30,000x,

6   100,000x and 300,000x. The diameters of at least 200 particles in each sample were then determined on

7   the micrographs with 300,000x magnification using the computer software Digital Micrograph (Gatan

8   Inc.).

9   *2.4.4 Asymmetric flow field-flow fractionation (FlFFF)*

10   The hydrodynamic diameter distributions of selected AgNP batches (Table 1), were determined within

11   one week of preparation by FlFFF, using an AF2000 instrument (Postnova Analytics) following the

12   method of Römer, et al. [26] and Baalousha and Lead [28]. The FlFFF channel featured a 1 kDa regenerated

13   cellulose ultrafiltration membrane (Postnova Analytics) with a 0.01 M $NaNO_3$ carrier solution. The AgNPs

14   were fractionated with cross-flow and detector flow both set to 1 mL min^{-1}, and their elution from the

15   FlFFF channel was monitored by UV-absorbance measurements at 254 nm (Postnova Analytics). The

16   FlFFF channel thickness was calibrated by analyzing polystyrene latex standards with known diffusion

17   coefficients under the same flow conditions as the AgNPs, and the diffusion coefficient distributions of

18   the AgNPs were thereafter calculated using FlFFF theory [29]. The hydrodynamic diameter distributions

19   were calculated from diffusion coefficients with the Stokes-Einstein equation.

20   *2.4.5 Yield determination*

21   To assess synthesis yields, 10 µl aliquots of 24 particle suspensions were dissolved in concentrated

22   HNO_3 and refluxed on a hotplate at 80°C for 48 hours to ensure complete dissolution. The resulting

23   solutions were evaporated to dryness and re-dissolved in 0.1 M HNO_3. Aliquots of these stock solutions

24   were then used to prepared more dilute 0.1 M HNO_3 'measuring' solutions that featured Ag

25   concentrations of about 20 ng mL^{-1} and that were doped with Pd as an internal standard, also at 20 ng

26   mL^{-1}. The technique of internal standardization, as opposed to an isotope dilution protocol, was applied

27   for quantification because the former produces sufficiently accurate and precise data (about ± 1 to 2%)

28   and its application is very straightforward for analyses of both labeled and unlabeled materials.

29   For quantification, the samples were analyzed relative to a standard solution with Ag and Pd abundances

30   of 20 ng mL^{-1} in the same acid matrix, using a Nu Plasma multiple collector ICP-MS (MC-ICP-MS)

31   instrument at the Imperial College MAGIC Laboratories. In these analyses the total Ag (^{107}Ag + ^{109}Ag)

32   signal intensities obtained for samples were compared to the standard solution and ^{105}Pd was monitored

33   to correct for any drifts in instrumental sensitivity. The measurements provided the total Ag

34   concentrations of the solutions and the yields of the synthesis methods were then calculated based on (i)

35   the dilutions factors used for the preparation of the measuring solutions and (ii) the total mass of Ag used

36   for particle preparation.

1   *2.4.6 Dissolution behavior*

2   The dissolution of the AgNPs was assessed by equilibrium dialysis. To this end, a PE container was

3   filled with 500 mL of a suspension of 107-AgNP2-Oct-F in dilute-ASW, at a concentration of 0.9 mg L^{-1}

4   Ag and 3.9 mg L^{-1} sodium citrate. Two dialysis bags (1kDa MWCO) were filled with 25 mL of dilute-ASW

5   and immersed in the container. The container was thereafter kept in the dark to avoid Ag

6   photodecomposition and stirred continuously. Sample aliquots of 0.5 mL were taken from both the inside

7   and outside of the dialysis bags on 14 occasions over a period of 27 days. A control experiment to

8   assess how dissolved Ag behaves during dialysis was carried out under the same conditions with 1 mg

9   L^{-1} Ag from an aqueous solution of AgNO$_3$. The background Ag concentrations for both experiments were

10   assessed from representative samples of dilute-ASW. Following completion of the experiments, the Ag

11   concentrations of sample aliquots were determined at FENAC by graphite furnace atomic absorption

12   spectrometry (GFAAS, Perkin Elmer AAS600).

13   **3. Results & Discussion**

14   All information gathered from the characterization of the 18 batches of AgNPs that were prepared during

15   the study is summarized in Table 1 and discussed in the following.

16   *3.1 Size characterization of nanoparticles*

17   *3.1.1 DLS analyses*

18   The average hydrodynamic diameter measured by DLS on the freshly made particles deviates by less

19   than ± 20% from the target size, with the exception of three batches (Nat-AgNP1-May12-F, 107-AgNP3-

20   May12-F, and 107-AgNP3-Oct12-F), where the average diameter was 40 to 70% larger than the target

21   size (Table 1).

22   In the following, we present and discuss the results of a statistical evaluation that interrogates whether

23   isotopic labeling or other factors (e.g., date or laboratory of synthesis) had a significant impact on the

24   size of the prepared AgNPs. In order to incorporate all particle suspensions in this evaluation, including

25   batches with different target sizes, we adopted the following procedure:

26   (i) All particle suspensions were split into one of three groups depending on their target particle size (17,

27   20 and 30nm). For each individual batch, the proportional difference from the mean size (PDMS) of

28   the group was calculated. This was achieved by finding the mean particle size (MS), as determined

29   by DLS, for each group. The particle size determined for an individual suspension (SamS) was then

30   subtracted from the mean value, to calculate the absolute difference between the individual and

31   mean particle sizes. The proportional difference was then determined by dividing the absolute

32   difference by the mean particle size (equation 1, Table 1, see supplementary material).

33       $$PDMS = (MS - SamS) / MS \qquad\qquad (1)$$

34   This normalization procedure was validated by t-tests that, where possible, were carried out using

35   both measured absolute size data and the calculated relative size differences. Specifically, this was

1   possible when the DLS sizes of Nat-AgNPs were compared with 107-AgNPs for each of the three

2   target sizes (30 nm, 20 nm, 17 nm; Table 1) Notably, these three t-tests yielded exactly identical

3   results when they were conducted with both the absolute and the normalized size data (see

4   supplementary material). This result validates the application of the normalized particles size data

5   (obtained as detailed above) in further t-tests.

6   (ii) The PDMSs calculated for each individual particle suspension were pooled in different manners to

7   produce populations that were evaluated using a Student's t-test. These tests evaluated whether

8   there are significant and systematic differences in size that can be assigned to a specific factor (see

9   supplementary material).

10   Based on two-tailed t-tests for populations of unequal variance, there was no significant difference at the

11   95% confidence level ($p = 0.05$) when the PDMSs were grouped into the following populations; (i) Nat-

12   AgNPs and labeled 107-AgNPs ($p = 0.57$), (ii) synthesis at the FENAC and Imperial College laboratories

13   ($p = 0.18$), (iii) synthesis date (e.g., May12-F, May12-IC and Oct12-F; $p = 0.27$ to 0.73), (iv) NP

14   preparation by operators AL and BS (particle synthesis in May and October 2012 respectively; $p = 0.45$),

15   and (v) freshly prepared and aged particles after 6-12 months storage ($p = 0.98$). These results were

16   obtained with the omission of batches 107-AgNP1-May12-F and 107-AgNP3-Oct12-F, which have

17   particularly anomalous sizes of 41.6 nm (target size 30 nm) and 28.1 nm (target size 17 nm),

18   respectively. These unusually large deviations from the target size may reflect experimental problems

19   during synthesis. However, very similar results are produced when these data are included in the above

20   t-test evaluations. A detailed summary of the t-test data and calculated p-values is presented in the

21   supplementary material.

22   Notably, the average particle diameters of the suspensions after storage deviated by less than 3.5 nm

23   from the average diameters that were measured directly after preparation. The only exception is sample

24   Nat-AgNP3-Oct-F, where the average diameter increased by about 90% (15.3 nm; Table 1). The PDIs

25   determined by DLS were less than 0.45 for all AgNP suspensions and less than 0.3 for 16 of the 18

26   batches, indicating that the particle size distributions were fairly monodisperse (Table 1). A t-test

27   demonstrated that there was no significant difference between the PDIs of (i) Nat-AgNPs and 107-

28   AgNPs ($p = 0.59$) and (ii) pristine particles and particles after storage ($p = 0.65$) (see supplementary

29   material).

30   Whilst the t-tests discussed above indicate that there are no statistically significant differences in

31   particles size and PDI that can be assigned to a single factor, the data of Table 1 nonetheless

32   demonstrate small but resolvable differences in particle size for NP batches prepared with the same

33   protocol. Given the results of the t-tests, these disparities most likely reflect 'normal' batch-to-batch

34   variations that occur, if syntheses are carried out on different days, in different laboratories and by

35   different operators. These results hence provide an indication of the particle size variability that can be

36   expected if different scientists apply the protocols of Table 2 in their own laboratories. In contrast, Römer,

37   et al. [26] previously demonstrated that, using similar protocols for the preparation of AgNPs, repeated

38   synthesis by the same operator, in the same laboratory with the same equipment and reagents, can

1   routinely provide particle batches with highly reproducible sizes. In summary, these results thus

2   demonstrate that despite small batch-to-batch variations in particles size that reflect slight differences in

3   experimental conditions, the protocols summarized in Table 2 are suitable for the robust and reliable

4   synthesis of AgNPs in different laboratories.

5   *3.1.2 TEM analyses*

6   Selected freshly prepared AgNP batches (Table 1) were imaged by TEM and evaluated by measuring

7   the longest axis of discrete particles rather than their aggregates (Table 1, Fig. 2). The TEM micrographs

8   show that the particles were spherical in shape and had a consistent size distribution, with the standard

9   deviation of all batches being 40 to 45% of the average particle diameter, equivalent to coefficients of

10 variance of 0.29-0.31 [30] (Table 1). It is likely that the aggregation of particles seen in the micrographs

11 occurred during drying of the samples on the TEM grids and is not due to the fusion of particles during

12 synthesis. This conclusion is supported by the predominance of discrete particles in suspension, as

13 indicated by the DLS results.

14 The average diameters determined from the TEM micrographs were typically 10 to 15% (about 3 - 4 nm)

15 smaller than the average hydrodynamic diameters determined by DLS. This is a well-known

16 phenomenon, which reflects that larger particles scatter proportionally more light, such that the average

17 DLS particle diameters are biased towards larger values [28]. The exceptions to this are samples Nat-

18 AgNP3-Oct12-F and 107-AgNP3-Oct12-F. The Nat-AgNP3-Oct12-F particle batch shows an average

19 TEM particle size that is very close to that determined by DLS, whereas there is a large discrepancy

20 between the DLS (28.1 nm) and TEM (16.3 nm) size data for 107-AgNP3-Oct12-F. These observations

21 are likely a consequence of the polydispersity of the respective samples. In particular, the particle size

22 distribution histogram of Nat-AgNP3-Oct12-F shows the smallest size range (Fig. 2), suggesting it is

23 highly monodisperse and therefore the DLS analysis shows very little size bias. In contrast, 107-AgNP3-

24 Oct12-F is the most polydisperse sample (PDI = 0.44), and this may reflect a small number of larger

25 particles in the suspension that heavily bias the DLS measurement.

26 *3.1.2 FIFFF analyses*

27 The FIFFF analysis [31, 32] of selected AgNP samples provided full width at half maximum (FWHM) data for

28 particle batches Nat-AgNP1-May12-F (24 nm), 107-AgNP1-May12-F (26 nm), Nat-AgNP2-May12-F (18

29 nm), 107AgNP2-May12-F (17 nm) and Nat-AgNP3-May12-F (11nm) (Fig. 3, Table 1). In addition, the

30 FIFFF data were used to determine the number average hydrodynamic diameters (d_n), weighted average

31 hydrodynamic diameters (d_w) and polydispersity (*PD*) using equations 2, 3 and 4, respectively, with

32 results given in Table 1.

33 $d_n = \Sigma_i C_i X_i / \Sigma_i C_i$ (2)

34 $d_w = \Sigma_i C_i X_i^2 / \Sigma_i C_i X_i$ (3)

35 $PD = d_w / d_n$ (4)

1   Here, C_i is the UV-absorbance signal at a given hydrodynamic diameter, X_i. The d_n values were typically

2   slightly smaller (up to 13%) whilst d_w was slightly larger (up to 32%) compared to the particle size

3   determined by DLS. The d_n values for 107-AgNP2-May12-F (17 nm) and Nat-AgNP2-May12-F (18 nm)

4   were only slightly larger than for Nat-AgNP3-May12-F (16 nm). The two former samples also showed a

5   higher PD value than Nat-AgNP3-May12-F, with size distributions tailing towards larger diameters (Fig.

6   3). As a consequence, there is a slightly lager difference in d_w values between 107-AgNP2-May12-F (22

7   nm) and Nat-AgNP2-May12-F (21 nm) versus Nat-AgNP3-May12-F (18 nm).

8   *3.2 Synthesis yields*

9   Reliable small-scale synthesis techniques with high yields are required for the production of isotopically

10   labeled NPs, due to the expense of using enriched stable isotopes (e.g., about \$3.50 per mg for [107]Ag

11   purchased from Isoflex USA in February 2012). The total Ag concentrations of 24 different particle

12   suspensions, encompassing 16 batches of labeled [107]AgNPs and 8 batches of non-labeled AgNPs, were

13   determined to assess the yield of the synthesis protocols (Table 1). Typically the yields were between

14   60% and 98%, with an average of 78% ± 23% (1sd). Considering that only small amounts of [107]Ag are

15   required for a single synthesis (~2.7 mg) and due to the excellent yields achieved here, the preparation

16   of [107]AgNPs is quite affordable, with a cost of approximately \$4 to \$5 per milligram.

17   *3.3 Dissolution behavior*

18   The results of the dialysis experiments are shown in Fig. 4. The particle stock suspension was added

19   directly to the dilute-ASW without prior treatment or washing to remove excess sodium citrate. Although

20   this effect was not investigated, the presence of sodium citrate at the expected concentration of ~4 mg L$^-$

21   ^{1} is not anticipated to have a significant influence on the dissolution behavior. The Ag contents measured

22   on the outside of the dialysis bags represent the total Ag concentration of the dilute-ASW, encompassing

23   both particulate and dissolved forms of Ag. In contrast, the Ag measured inside the bags has crossed a

24   1kDa MWCO dialysis membrane and therefore reflects the dissolved component only. The experimental

25   setup therefore ensures that identical Ag concentrations for the dialysis bags and the container are only

26   achieved, when all Ag in the latter reservoir is in dissolved form.

27   The dialysis control experiment, where 1.00 mg L^{-1} of aqueous Ag was introduced into the containers,

28   can be used to assess the behavior of dissolved Ag in the absence of AgNPs. At the beginning of the

29   control experiment, the Ag concentrations inside the dialysis bags increased rapidly and reached the

30   same level (of about 0.8-1.1 mg L^{-1}) as on the outside after 8 hours, demonstrating the time required for

31   equilibrium to establish over the dialysis membrane (Fig. 4a). During the remaining 27 days of the

32   experiment, the Ag concentrations inside and outside the dialysis bags were always essentially identical,

33   and this shows that the setup functioned well to provide a reliable monitor of dissolved Ag contents on

34   the outside of the dialysis bags. However, the Ag concentration outside the bags decreased during most

35   of the experiment to a value of about 0.4 mg L^{-1} after 22 days. This indicates that dissolved Ag was lost,

36   presumably as a result of adsorption onto the container walls and the dialysis membrane. The small final

1   increase in dissolved Ag concentration that is seen at day 27, is likely due to desorption of the Ag from

2   the surfaces of the container and dialysis bags.

3   In the dialysis experiment of sample 107-AgNP2-Oct12-F, the Ag concentration outside the bags

4   immediately after NP addition was 0.5 mg L^{-1}, a recovery of only 56% (Fig. 4b). The container was

5   furthermore black in color after the addition of the ^{107}AgNPs, which indicates that AgNP adsorption to

6   container surfaces was responsible for the loss of Ag. During the experiment, the Ag concentration

7   outside of the bags generally decreased until day 22. For the same time period, the Ag contents inside

8   both dialysis bags initially showed an increase over the first 28 hours, followed by a decrease until day 8,

9   with increasing concentrations observed thereafter (Fig. 4b). On day 22, the Ag concentrations outside

10   and within both dialysis bags were identical and all three concentrations rose continuously during the

11   final time period to day 27. This final increase in concentration is similar to that seen in the control

12   experiment, which suggests that it is also most likely caused by desorption of Ag from surfaces that are

13   in contact with the dilute-ASW.

14   Due to the adsorptive losses of both dissolved and nanoparticulate Ag during dialysis, it is difficult to

15   quantify the dissolution behavior of the AgNPs. It may be assumed, however, that the dissolution of

16   AgNPs will be similar, regardless of whether they are in suspension or adsorbed to container walls. With

17   this assumption, our data can be applied to derive some general conclusions about the dissolution

18   behavior of AgNPs. In particular, after an initial 8-hour equilibration time, the control experiment with

19   dissolved Ag exhibited nearly identical Ag concentrations inside and outside of the dialysis bags (Fig. 4a).

20   During the same time period, the dialysis experiment with NP sample 107-AgNP2-Oct12-F showed low

21   Ag concentrations inside the dialysis bags (0.02-0.04 mg L^{-1}), which correspond to only 2-5% of the

22   ^{107}AgNP concentration that was initially added to the container (Fig. 4b). These observations indicate that

23   the ^{107}AgNP suspension in dilute-ASW produced only a very small fraction of dissolved Ag during the first

24   few hours of the experiment. Over the following 27 days of the ^{107}AgNP dialysis experiment, the Ag

25   concentrations inside the dialysis bags displayed an overall increase, demonstrating extensive ^{107}AgNP

26   dissolution (Fig. 4b). This conclusion is supported by the observation that very similar Ag concentrations

27   were observed for the inside and outside of the dialysis bags on day 27, with a final Ag concentrations of

28   0.32 mg L^{-1} for both bags (Fig. 4b). As some dissolved Ag was probably lost to adsorption onto the

29   container walls, the value of 0.32 mg L^{-1} can be taken to represent a tentative minimum estimate for the

30   solubility of the ^{107}AgNPs in dilute ASW. Given the adsorption problems encountered here with the

31   dialysis technique, future AgNP dissolution studies should consider using alternative methods, such as

32   ultrafiltration, to obtain improved constraints on the dissolution behavior of AgNPs.

33   *3.4 Reproducibility and reliability of synthesis method*

34   The three synthesis protocols produced fairly monodisperse AgNP suspensions throughout, but

35   suspensions prepared with the same protocol display small but significant batch-to-batch variations in

36   size, regardless of the isotopic composition of the AgNPs (Table 1). A detailed evaluation of the results

37   (Table 1) demonstrates, however, that the protocols for particle target sizes of 30 nm (AgNP1), 20 nm

38   (AgNP2) and 17 nm (AgNP3) still offer acceptable control on particle size. Protocol AgNP1 produced the

1   largest particles (26.5 – 31.2 nm, average = 30.7 ± 2.9 nm; 1sd, n = 5), whilst the particles from protocols

2   AgNP2 (16.3 – 23.9 nm, average = 19.6 nm ± 3.0 nm; 1sd, n = 6) and AgNP3 (17.1 – 24.3 nm, average

3   = 19.5 ± 2.7 nm; 1sd, n = 5) were smaller but similar. These quoted averages were calculated from all

4   DLS data obtained for freshly prepared particles (Table 1), excluding the two most obvious outliers (Nat-

5   AgNP1-May12-F and 107-AgNP3-Oct12-F), but very similar results are obtained when the complete

6   dataset is considered (see supplementary material).

7   These findings demonstrate that the methods provide a robust means of obtaining small batches of

8   isotopically labeled AgNPs with diameters that closely match desired target sizes. However, due to the

9   observed batch-to-batch variations in size, particle characterization will need to be carried out for

10 applications, which require that particles diameters are known to a high degree of accuracy. Although

11 only three synthesis protocols were utilized here, it is likely that the experimental conditions can be

12 adjusted to target larger and smaller particle sizes. For example, slightly modified versions of the

13 synthesis methods applied here were used in previous studies to produce AgNPs with diameters as

14 small as 11.5 nm[33] and 7.2 nm[26] when measured by TEM.

15 *3.5 Stability of particles*

16 The particle suspensions in aqueous Na-citrate solutions were stored in the dark at 4°C to help prevent

17 ageing. To assess the stability of the particle suspensions under these conditions, a selection of particle

18 batches were characterized by DLS periodically during 12 months of storage (Table 1). Batch Nat-

19 AgNP3-Oct12-F showed the most significant signs of ageing, as after 6 months storage the average

20 particle size and PDI increased from 17.2 to 32.5 nm and from 0.25 to 0.52, respectively. Whilst this is

21 the type of change that would be expected as a result of particle aggregation, it was shown by Römer, et

22 al. [26] that small citrate-capped Ag NPs generally have a greater stability and exhibit less agglomeration

23 than larger particles. This indicates that the aggregation determined for sample Nat-AgNP3-Oct12-F may

24 be an atypical result. All other particle batches exhibited no significant signs of ageing with all but one

25 sample showing less than a 10% change in the average DLS particle size (Table 1). In addition, the PDI

26 data also display only minor changes, indicating that the particle suspensions remained fairly

27 monodisperse. The size and PDI results, furthermore, reveal no difference in aging behavior between

28 natural and isotopically labeled AgNPs (Table 1). Any changes that might occur to the stock suspensions,

29 such as agglomeration, may influence the particle behavior, but would have no effect on the isotope label

30 or tracing capabilities.

31 *3.6 Isotope label & detection capabilities*

32 The motivation for synthesizing AgNPs from enriched [107]Ag is to produce a material with a distinct non-

33 natural isotope signature, which can be used in experiments and exposures, so that changes induced in

34 the ^{107}Ag/^{109}Ag isotope ratio of relevant samples (e.g. biological materials, soil or water) can be used to

35 trace and quantify the presence of the labeled material [17, 18, 22, 23, 27] (Fig. 1). The contribution of enriched

36 ^{107}Ag to a sample is only detectable when the deviation induced in the ^{107}Ag/^{109}Ag ratio of the sample

1   clearly exceeds (i) the precision of the isotopic measurement or (ii) any natural variations in the isotope

2   composition of Ag. These factors are discussed below.

3   Isotopic analyses of Ag are generally carried out using ICP-MS instrumentation, as measurements by

4   thermal ionization mass spectrometry (TIMS) are significantly more cumbersome [34]. Using standard

5   quadrupole ICP-MS (Q-ICP-MS) instruments, $^{107}Ag/^{109}Ag$ ratios can typically be measured with a

6   precision of about 1–5% (2sd). Improved data with a precision of ±0.2 to 1% (2sd) can be obtained with

7   Q-ICP-MS at optimal analytical conditions (including separation of Ag from matrix elements) or by the

8   application of single collector sector field ICP-MS (SF-ICP-MS) [35]. Even more precise isotopic

9   measurements are possible by multiple collector ICP-MS (MC-ICP-MS), which can achieve uncertainties

10   of better than ±0.02% (2sd) for $^{107}Ag/^{109}Ag$ on purified solutions of Ag [36, 37].

11   Studies to investigate natural stable isotope fractionation of Ag are extremely limited in number and

12   scope, with a primary focus on Ag ores (which are straightforward to analyze) and a few igneous rocks

13   [38-40]. Data are also available from an archeological study on the provenance of coins [41] and an

14   investigation into natural isotope fractionation based on a limited number of environmental samples [42].

15   These analyses revealed only minor differences of about ±0.05% in the $^{107}Ag/^{109}Ag$ ratios of the samples,

16   relative to the NIST SRM 978a Ag isotope standard. Such small variations are only resolvable using MC-

17   ICP-MS and hence have no impact on the sensitivity that can be achieved for the detection of isotopically

18   labeled AgNPs by Q-ICP-MS and SF-ICP-MS. Given the published results, it is furthermore unlikely that

19   samples, such as soils or sediments, from a single location will exhibit geological Ag isotope

20   fractionations that exceed ±0.02% and hence impact the AgNP detection sensitivity of MC-ICP-MS.

21   However, there are currently no studies that investigate whether changes in Ag isotope composition are

22   generated by biological uptake and processing of this element. Based on data acquired for other

23   elements, such Zn [43] and Cd [44], it is conceivable that biotic reactions may induce Ag isotope effects in

24   the range of 0.02% to 0.05% and such fractionations may be preserved in biological tissue and fluids,

25   water samples or soils and sediments. It is unlikely, however, that biological isotope effects will normally

26   exceed 0.1% to 0.2% and hence no serious impact on the detection sensitivity of MC-ICP-MS for

27   isotopically labeled AgNPs is expected. Nonetheless, it will be important for future work to carefully

28   characterize possible biological Ag isotope fractionations. If natural Ag isotope variations of ≥0.05% are

29   found to be common and deemed to be obstructive, this problem can be readily circumvented by

30   analyses of appropriate control samples. Such measurements can characterize the natural Ag isotope

31   composition and variability of the background, and this permits appropriate corrections and/or

32   uncertainties to be applied to the isotopic data collected for exposed samples.

33   Ecotoxicology studies typically generate and require analyses for a large number of samples (more than

34   100), making it important to consider the balance between optimal data quality and high sample

35   throughput. Whilst MC-ICP-MS can provide unrivalled precision for the determination of $^{107}Ag/^{109}Ag$, such

36   analyses are also particularly laborious, because Ag must be separated from any sample matrix prior to

37   analysis. In contrast, quadrupole and sector field ICP-MS can be employed for direct $^{107}Ag/^{109}Ag$

38   measurements without chemical separation. As sample preparation is much more straightforward, the

1   latter instruments can achieve significantly higher sample throughput but at the cost of somewhat poorer

2   precision for the data, which ultimately limits the tracing capabilities.

3   In the following, we discuss the tracing sensitivities that can be achieved using labeled ^{107}Ag (and thus

4   ^{107}AgNPs) for two hypothetical cases with relevance to ecotoxicology, and where the endmember

5   methods of Q-ICP-MS and MC-ICP-MS are evaluated for detection (Table 3). Case 1 involves analyses

6   of 5 mg dry weight samples of biological tissue, as might be obtained from invertebrates following

7   exposures, with a realistic Ag background of 100 ng g^{-1} [5]. Case 2 is for a 5 mL water sample (a realistic

8   volume for removal and analysis from a laboratory exposure) that features a Ag background

9   concentration of 200 ng L^{-1}, as would be appropriate for river, lake and estuarine waters [5]. Based on the

10   concentrations quoted above, the Case 1 and 2 samples would contain only 0.5 ng and 1 ng of Ag,

11   respectively (Table 3), and these small amounts will limit the precision of the isotopic analyses by ICP-

12   MS. Based on literature data and test measurements conducted at Imperial College (for MC-ICP-MS), it

13   is estimated that the diagnostic ^{107}Ag/^{109}Ag isotope ratio can be determined in these samples with a

14   precision of about ±5% for Q-ICP-MS and ± 0.05% for MC-ICP-MS (an intermediate precision is

15   expected for SF-ICP-MS).

16   The precision of mass spectrometric measurements is defined here as the 2sd calculated from replicate

17   isotope analyses of samples or a standard reference material. The analytical precision is a key factor

18   because it determines the smallest change in the ^{107}Ag/^{109}Ag isotope ratio (ΔR_{res}), as induced by addition

19   of the ^{107}Ag tracer, which is analytically resolvable as a deviation from the natural ^{107}Ag/^{109}Ag (R_{nat})_ratio,

20   such that ΔR_{res} = 2sd.

21   The addition of an enriched ^{107}Ag tracer to a natural sample will increase the ^{107}Ag/^{109}Ag ratio of the

22   system. In the following, we define R_{res}, as the ^{107}Ag/^{109}Ag ratio, which is associated with the smallest

23   addition of ^{107}Ag tracer that is resolvable by measurement. R_{res} is therefore given by:

24   $$R_{res} = R_{nat} + \Delta R_{res} \tag{5}$$

25   Isotope mass balance can then be used to calculate the minimum molar amount of enriched ^{107}Ag (N_{res}-

26   Ag$_{en}$), from labeled ^{107}AgNPs, that must be added to a given molar amount of natural Ag (N-Ag$_{nat}$) in a

27   system, to increase the ^{107}Ag/^{109}Ag ratio from R_{nat} to R_{res}:

28   $$N_{res}\text{-}Ag_{en} = N\text{-}Ag_{nat} \times ((R_{res} \times {}^{109}Ab_{nat}) - {}^{107}Ab_{nat}) / ({}^{107}Ab_{en} - (R_{res} \times {}^{109}Ab_{en})) \tag{6}$$

29   where the fractional (molar) isotope abundances of ^{107}Ag and ^{109}Ag in the enriched material (^{107}Ab$_{en}$ and

30   ^{109}Ab$_{en}$) and natural Ag (^{107}Ab$_{nat}$ and ^{109}Ab$_{nat}$) are 99.2%, 0.8% and 51.8%, 48.2%, respectively. Equation

31   (6) can be readily revised to determine the minimum molar concentration [N_{res}-Ag$_{en}$] of enriched ^{107}Ag

32   that must be added to obtain R_{res} – this requires only that N-Ag$_{nat}$ is substituted with the molar

33   concentration of natural Ag, [N-Ag$_{nat}$]. Given that the atomic weights of natural and enriched Ag differ by

34   less than 1%, Equation 6 also provides a sufficiently accurate approximation for calculation of the

35   minimum masses and mass concentrations of enriched ^{107}Ag, which must be added to the system, to

36   achieve a detectable change in the final ^{107}Ag/^{109}Ag ratio.

1   The final ^{107}Ag/^{109}Ag isotope ratio of an exposed sample (R_{sam}), as measured by ICP-MS, is used to

2   quantify the amount of enriched ^{107}Ag label present. This calculation is outlined in the following. The

3   molar fraction of enriched ^{107}Ag to total Ag (fr_{en}) present in the sample is given by:

4    $$fr_{en} = N\text{-}Ag_{en} / (N\text{-}Ag_{nat} + N\text{-}Ag_{en}) \qquad (7)$$

5   where $N\text{-}Ag_{en}$ is the molar amount of enriched ^{107}Ag tracer present. Using R_{sam}, fr_{en} can be determined

6   as:

7    $$fr_{en} = [(^{107}Ab_{en} - (R_{sam} \times {}^{109}Ab_{en})) / ((R_{sam} \times {}^{109}Ab_{nat}) - {}^{107}Ab_{nat}) + 1]^{-1} \qquad (8)$$

8   The fractional molar abundance of ^{109}Ag in the exposed sample ($^{109}Ab_{sam}$) is then:

9    $$^{109}Ab_{sam} = (fr_{en} \times {}^{109}Ab_{en}) + ((1 - fr_{en}) \times {}^{109}Ab_{nat}) \qquad (9)$$

10   The molar abundance of total Ag (N-Ag) and enriched Ag ($N\text{-}Ag_{en}$) in the sample can be determined by

11   quantifying $N\text{-}^{109}Ag$, the molar amount of ^{109}Ag present. This can be readily achieved using standard

12   ICP-MS techniques, where a solution prepared from a known aliquot of the sample is analyzed, such that

13   $N\text{-}^{109}Ag$ can be determined relative to a suitable calibration curve. Following this, N-Ag and $N\text{-}Ag_{en}$ can

14   be calculated from:

15   $$N\text{-}Ag = (N\text{-}^{109}Ag / {}^{109}Ab_{sam}) \qquad (10)$$

16   $$N\text{-}Ag_{en} = (N\text{-}^{109}Ag / {}^{109}Ab_{sam}) \times fr_{en} \qquad (11)$$

17   The mass $M\text{-}Ag_{en}$ and mass concentration $[M\text{-}Ag_{en}]$ of enriched Ag in the sample can then be obtained

18   as:

19   $$M\text{-}Ag_{en} = N\text{-}Ag_{en} \times AtW_{en} \qquad (12)$$

20   $$[M\text{-}Ag_{en}] = (N\text{-}Ag_{en} \times AtW_{en}) / M \qquad (13)$$

21   where M is the sample mass. The atomic weight of the enriched Ag, AtW_{en}, can be determined from:

22   $$AtW_{en} = (^{107}Ab_{en} \times {}^{107}AtW) + (^{109}Ab_{en} \times {}^{109}AtW) \qquad (14)$$

23   where ^{107}AtW and ^{109}AtW are the known atomic weights of ^{107}Ag and ^{109}Ag. Calculations analogous to

24   those performed in Equations 12 to 14 can be used to derive the total mass of Ag in the sample (M-Ag)

25   and the Ag mass concentration [M-Ag].

26   The results of these calculations for Cases 1 and 2 are given in Table 3. In detail, they indicate that

27   isotopic tracing with Q-ICP-MS requires that the addition of enriched ^{107}Ag raises the total Ag

28   concentration by at least 2.6%, to 102.6 ng g^{-1} for the tissue (Case 1) and 205 ng L^{-1} for the water

29   sample (Case 2; Table 3). With MC-ICP-MS, measurements of the ^{107}Ag/^{109}Ag ratio are about 100-fold

30   more precise and consequently the tracing sensitivity is also improved by two orders of magnitude. In

31   this scenario the Ag sample concentration only needs to increase by 0.026% from the addition of ^{107}Ag,

1   to generate analytically resolvable differences in the $^{107}Ag/^{109}Ag$ ratio. For the tissue and water samples,

2   this means that increases in the Ag concentration to 100.026 ng g^{-1} (from 100 ng g^{-1}) and 200.05 g L^{-1}

3   (from 200 g L^{-1}), respectively, are already traceable by isotopic analyses. Evaluation of the detection

4   sensitivity for a given isotope label, analytical approach and natural background concentration in this

5   manner, enables appropriate experimental plans and dosing levels to be prepared.

6   The uncertainties of the isotope ratio analyses can be propagated through the above equations to

7   assess the impact of the measurement precision on the calculated mass of enriched tracer material

8   present in a sample or its mass concentration. Importantly, the uncertainties do not scale in a linear

9   manner and depend on the isotopic enrichment of the tracer and the proportion of enriched to natural Ag

10   in the sample. To demonstrate this, the uncertainties for [M-Ag$_{en}$] of Cases 1 and 2 (Table 3) were

11   calculated for the addition of ^{107}Ag-enriched tracer at levels, which exceed the smallest detectable molar

12   concentration N$_{res}$-Ag$_{en}$ by a factor of 10x and 100x.

13   The results of these calculations are promising because they indicate that despite of the unfavorable

14   natural isotope composition of Ag, stable isotope labeling of Ag can provide detection sensitivities and

15   uncertainties of quantification that are far better than those achievable by concentration tracing.

16   Considering that the latter methodology can only provide unequivocal results if the concentration

17   anomalies generated by elemental uptake exceed the natural background levels by at least a factor of 2

18   (but preferably more), the application of stable isotope labeling enhances the tracing sensitivity by a least

19   a factor of 40 (using Q-ICP-MS for detection) and possibly by up to a factor of ~4000 (with use of MC-

20   ICP-MS). Furthermore, with the superior precision of MC-ICP-MS for isotopic analyses, the tracing

21   sensitivities are likely to be sufficiently high, to enable experiments to be carried out at low and

22   environmentally relevant exposure concentrations.

23   **4. Conclusions**

24   In this study, published methods were modified for small-scale synthesis of citrate-capped AgNPs from

25   both natural Ag and enriched ^{107}Ag. Three different synthesis protocols were used on three occasions

26   and in two laboratories to obtain AgNPs with target sizes of 17, 20 and 30 nm. All particles batches

27   produced were thoroughly characterized and the results demonstrate that the new procedures provide

28   reproducible, monodisperse particle suspensions at high yields of ~80% and with a long-term stability of

29   up to 12 months. Whilst the measurements revealed small but significant batch-to-batch variations in

30   size, the particles were generally found to have diameters that closely matched the desired target sizes.

31   Detailed statistical tests furthermore argue against systematic differences in size between AgNPs

32   prepared from enriched ^{107}Ag versus natural Ag. In summary, these results show that the new methods

33   are ideally suited for the small-scale preparation of isotopically labeled AgNPs. Simple isotope mass

34   balance calculations furthermore demonstrate that application of stable isotope labeling can increase the

35   detection sensitivity of AgNPs in environmental samples by at least a factor of 40 and possibly by up to

36   4000x, in comparison to commonly employed bulk Ag concentration measurements. Use of the most

37   precise isotopic measurement techniques should therefore, permit environmentally realistic exposure

38   scenarios.

1   **Acknowledgements**

10

11   **References**

12   1.   T. W. Purcell and J. J. Peters, *Environ Toxicol Chem*, 1998, 17, 539-546.
13   2.   S. W. P. Wijnhoven, W. J. G. M. Peijnenburg, C. A. Herberts, W. I. Hagens, A. G. Oomen, E. H.
14   W. Heugens, B. Roszek, J. Bisschops, I. Gosens, D. Van de Meent, S. Dekkers, W. H. De Jong,
15   M. Van Zijverden, A. J. A. M. Sips and R. E. Geertsma, *Nanotoxicology*, 2009, 3, 109-138.
16   3.   Woodrow Wilson consumer products inventory for products containing nano-silver,
17   http://www.nanotechproject.org/cpi/browse/nanomaterials/silver-nanoparticle/, Accessed
18   December 2013.
19   4.   F. Gottschalk, T. Sun and B. Nowack, *Environmental pollution*, 2013, 181, 287-300.
20   5.   R. Eisler, *Silver hazards to fish, wildlife and invertebrates: A synoptic review*, U.S. Department of
21   the Interior, 1996.
22   6.   W. A. Shoults-Wilson, B. C. Reinsch, O. V. Tsyusko, P. M. Bertsch, G. V. Lowry and J. M. Unrine,
23   *Soil Sci Soc Am J*, 2011, 75, 365-377.
24   7.   C. M. Zhao and W. X. Wang, *Environ Toxicol Chem*, 2011, 30, 885-892.
25   8.   L. Maretti, P. S. Billone, Y. Liu and J. C. Scaiano, *J Am Chem Soc*, 2009, 131, 13972-13980.
26   9.   T. Xia, M. Kovochich, M. Liong, L. Madler, B. Gilbert, H. B. Shi, J. I. Yeh, J. I. Zink and A. E. Nel,
27   *Acs Nano*, 2008, 2, 2121-2134.
28   10.   A. Chrastina and J. E. Schnitzer, *Int J Nanomed*, 2010, 5, 653-659.
29   11.   C. Coutris, E. J. Joner and D. H. Oughton, *Sci Total Environ*, 2012, 420, 327-333.
30   12.   M. Zuykov, E. Pelletier and S. Demers, *Mar Environ Res*, 2011, 71, 17-21.
31   13.   N. Lewinski, V. Colvin and R. Drezek, *Small*, 2008, 4, 26-49.
32   14.   T. Tenuta, M. P. Monopoli, J. Kim, A. Salvati, K. A. Dawson, P. Sandin and I. Lynch, *Plos One*,
33   2011, 6.
34   15.   N. Gibson, U. Holzwarth, K. Abbas, F. Simonelli, J. Kozempel, I. Cydzik, G. Cotogno, A.
35   Bulgheroni, D. Gilliland, J. Ponti, F. Franchini, P. Marmorato, H. Stamm, W. Kreyling, A. Wenk,
36   M. Semmler-Behnke, S. Buono, L. Maciocco and N. Burgio, *Arch Toxicol*, 2011, 85, 751-773.
37   16.   D. H. Oughton, T. Hertel-Aas, E. Pellicer, E. Mendoza and E. J. Joner, *Environ Toxicol Chem*,
38   2008, 27, 1883-1887.
39   17.   F. R. Khan, A. Laycock, A. Dybowska, F. Larner, B. D. Smith, P. Rainbow, S. N. Luoma, M.
40   Rehkämper and E. Valsami-Jones, *Environ Sci Technol*, 2013, 47, 8532-8439.
41   18.   F. Larner, Y. Dogra, A. Dybowska, J. Fabrega, B. Stolpe, L. J. Bridgestock, R. Goodhead, D. J.
42   Weiss, J. Moger, J. R. Lead, E. Valsami-Jones, C. R. Tyler, T. S. Galloway and M. Rehkämper,
43   *Environ Sci Technol*, 2012, 46, 12137-12145.
44   19.   N. A. Matwiyoff and D. G. Ott, *Science (New York, N Y)*, 1973, 181, 1125-1133.
45   20.   C. Sridar, I. Hanna and P. F. Hollenberg, *Xenobiotica*, 2013, 43, 336-345.
46   21.   S. K. Misra, A. Dybowska, D. Berhanu, M. N. Croteau, S. N. Luoma, A. R. Boccaccini and E.
47   Valsami-Jones, *Environ Sci Technol*, 2012, 46, 1216-1222.
48   22.   M. N. Croteau, A. D. Dybowska, S. N. Luoma and E. Valsami-Jones, *Nanotoxicology*, 2011, 5,
49   79-90.
50   23.   B. Gulson, M. McCall, M. Korsch, L. Gomez, P. Casey, Y. Oytam, A. Taylor, M. McCulloch, J.
51   Trotter, L. Kinsley and G. Greenoak, *Toxicol Sci*, 2010, 118, 140-149.

1   24.   J. Gigault and V. A. Hackley, *Analytica Chimica Acta*, 2013, 763, 57-66.
2   25.   S. A. Cumberland and J. R. Lead, *J Chromatogr A*, 2009, 1216, 9099-9105.
3   26.   I. Römer, T. A. White, M. Baalousha, K. Chipman, M. R. Viant and J. R. Lead, *J Chromatogr A*,
4   2011, 1218, 4226-4233.
5   27.   F. Larner and M. Rehkämper, *Environ Sci Technol*, 2012, 46, 4149-4158.
6   28.   M. Baalousha and J. R. Lead, *Environ Sci Technol*, 2012, 46, 6134-6142.
7   29.   A. Litzen, *Anal Chem*, 1993, 65, 461-470.
8   30.   M. Baalousha and J. R. Lead, *Nat Nanotechnol*, 2013, 8, 308-309.
9   31.   M. Baalousha and J. R. Lead, *Environ Sci Technol*, 2007, 41, 1111-1117.
10   32.   M. Baalousha, A. Manciulea, S. Cumberland, K. Kendall and J. R. Lead, *Environ Toxicol Chem*,
11   2008, 27, 1875-1882.
12   33.   M. Tejamaya, I. Römer, R. C. Merrifield and J. R. Lead, *Environ Sci Technol*, 2012, 46, 7011-
13   7017.
14   34.   J. H. Chen and G. J. Wasserburg, *Geochim Cosmochim Ac*, 1990, 54, 1729-1743.
15   35.   K. G. Heumann, S. M. Gallus, G. Radlinger and J. Vogl, *J Anal Atom Spectrom*, 1998, 13, 1001-
16   1008.
17   36.   M. Schönbächler, R. W. Carlson, M. E. Horan, T. D. Mock and E. H. Hauri, *International Journal*
18   *of Mass Spectrometry*, 2007, 261, 183-191.
19   37.   S. J. Woodland, M. Rehkämper, A. N. Halliday, D. C. Lee, B. Hattendorf and D. Gunther,
20   *Geochim Cosmochim Ac*, 2005, 69, 2153-2163.
21   38.   A. V. Chugaev and I. V. Chernyshev, *Geochem Int+*, 2012, 50, 899-910.
22   39.   E. Hauri, R. Carlson and J. Bauer, 2000.
23   40.   S. J. Woodland, M. Rehkämper, D. C. Lee and A. N. Halliday, *Geochim Cosmochim Ac*, 2002,
24   66, A847-A847.
25   41.   A. M. Desaulty, P. Telouk, E. Albalat and F. Albarede, *P Natl Acad Sci USA*, 2011, 108, 9002-
26   9007.
27   42.   Y. Luo, E. Dabek-Zlotorzynska, V. Celo, D. C. G. Muir and L. Yang, *Anal Chem*, 2010, 82, 3922-
28   3928.
29   43.   T. Arnold, M. Schönbächler, M. Rehkämper, S. Dong, F. J. Zhao, G. J. Kirk, B. J. Coles and D. J.
30   Weiss, *Anal Bioanal Chem*, 2010, 398, 3115-3125.
31   44.   S. Ripperger, M. Rehkämper, D. Porcelli and A. N. Halliday, *Earth Planet Sc Lett*, 2007, 261,
32   670-684.

33

1 **Table 1.** Summary of characterization data obtained for batches of [107]AgNPs and natural AgNPs prepared on three different occasions using the three
2 synthesis protocols. Results are shown for both pristine particles and after up to 12 months of storage

					Freshly Prepared Particles						Particles after Storage		
		DLS		**TEM**			**FIFFF**					**DLS**	
Particle Batch[a]	Yield (%)	Diameter[b] (nm)	PDI[c]	Diameter[d] (nm)	CV[ce]	d_n[f] (nm)	d_w[g] (nm)	PD[h]	FWHM[i] (nm)	Storage[j] (Months)	Diameter[d] (nm)	PDI[e]
AgNP1 protocol – target particle size 30 nm												
Nat-AgNP1-May12-F	91	41.6	0.25			36	49	1.3	24	12	41.5	0.25
107-AgNP1-May12-F	64	29.3	0.22			27	31	1.2	26	12	29.7	0.20
Nat-AgNP1-May12-IC	14	35.5	0.26							12	35.3	0.23
107-AgNP1-May12-IC		31.2	0.16									
Nat-AgNP1-Oct12-F	79	26.5	0.13	22.3 ± 6.7	0.30					6	26.8	0.11
107-AgNP1-Oct12-F	98	31.2	0.18	28.2 ± 8.3	0.29					6	33.7	0.22
AgNP2 protocol – target particle size 20 nm												
Nat-AgNP2-May12-F	87	20.7	0.33			18	21	1.2	18	12	19.7	0.25
107-AgNP2-May12-F	83	16.7	0.25			17	22	1.3	17	12	14.6	0.34
Nat-AgNP2-May12-IC	61	17.2	0.28							8	16.8	0.35
107-AgNP2-May12-IC	61	16.3	0.27							12	17.5	0.18
Nat-AgNP2-Oct12-F	63	22.6	0.15	19.5 ± 5.7	0.29					6	22.9	0.10
107-AgNP2-Oct12-F	78	23.9	0.20	20.1 ± 6.3	0.31					6	24.1	0.18
AgNP3 protocol – target particle size 17 nm												
Nat-AgNP3-May12-F		17.1	0.20			16	18	1.1	11			
107-AgNP3-May12-F		24.3	0.24									
Nat-AgNP3-May12-IC	77	18.2	0.23							12	16.8	0.31
107-AgNP3-May12-IC	31	20.6	0.29							12	24.1	0.21
Nat-AgNP3-Oct12-F	80	17.2	0.25	18.0 ± 5.2	0.29					6	32.5	0.52
107-AgNP3-Oct12-F	76	28.1	0.44	16.3 ± 4.8	0.29					6	26.1	0.39

3 TEM - Transmission electron microscopy, CV – Coefficient of Variance, DLS - Dynamic light scattering, FIFFF – Asymmetric Flow Field Flow Fractionation, [a] Each particle
4 batch was designated depending on (i) whether the batch was labeled or non-labeled (107-AgNP or Nat-AgNP), (ii) which synthesis protocol was used for the production (1,
5 2 or 3; see Table 2), (iii) whether the particles were made in May or October 2012 (May12 or Oct12) and (iv) the laboratory in which the synthesis was carried out, either at
6 FENAC, University of Birmingham (F) or the MAGIC Laboratory, Imperial College London (IC). [b] The hydrodynamic diameter was calculated as the average of individual
7 DLS measurements. [c] Polydispersity index. [d] The average TEM diameter ± 1sd is calculated from analyses of 234 -337 individual particles. [e] CV = Standard deviation/TEM
8 diameter. [f] The number average hydrodynamic diameter. [g] The weighted average hydrodynamic diameter. [h] Polydispersity (d_n/d_f). [i] Full width at half maximum. [j] Particle
9 storage was in the dark at 4°C.
10

1   **Table 2.** Summary of AgNP synthesis protocols

Step	Synthesis protocol		
	AgNP1	AgNP2	AgNP3
Mix Na-citrate[1] & Ag-nitrate[2] solutions then stir for	10 min	10 min	10 min
Add 6 mL $NaBH_4$[3] solution	10 mM	1 mM	-
Boil mixture	90 min	90 min	90 min
Add 6 mL $NaBH_4$[3] solution	-	-	10 mM
Continue to boil	-	-	10 min
Allow to cool in the dark	RT[4]	RT[4]	RT[4]

2   [1] 100 mL of 0.30 mM Na-citrate solution in >18.2 MΩ cm water. [2] 100mL of
3   0.25 mM Ag-nitrate solution in >18.2 MΩ cm water. [3] Aliquot, with
4   appropriate dilution, of 100mL of 10mM $NaBH_4$ stock solution in >18.2 MΩ
5   cm water. [4] RT = Room temperature

6

7

8

9

10

11

12

13

14

15

16

17

18

19

20

21

22

23

24

25

26

27

28

1 **Table 3.** Summary of data for the hypothetical cases that evaluate the detection sensitivities and
2 quantification uncertainties achievable for tracing of highly enriched ^{107}Ag in environmental
3 samples

	Case1	Case 2
Sample	5 mg biological tissue	5 mL water
Background Ag concentration	100 ng g^{-1}	200 ng L^{-1}
Total natural Ag content of sample	0.5 ng	1 ng
Analysis by Q-ICP-MS, precision ±5% (2sd)		
Minimum concentration change detectable by ^{107}Ag/^{109}Ag analysis*	2.6 ng g^{-1}	5.2 ng L^{-1}
Uncertainty in quantification of label at:		
10x minimum concentration	126 ± 3.12 ng g^{-1}	252 ± 6.24 ng L^{-1}
100x minimum concentration	360 ± 4.37 ng g^{-1}	720 ± 8.76 ng L^{-1}
Analysis by MC-ICP-MS, precision ±0.05% (2sd)		
Minimum concentration change detectable by ^{107}Ag/^{109}Ag analysis*	0.026 ng g^{-1}	0.052 ng L^{-1}
Uncertainty in quantification of label at:		
10x minimum concentration	100.26 ± 0.026 ng g^{-1}	200.52 ± 0.053 ng L^{-1}
100x minimum concentration	102.6 ± 0.027 ng g^{-1}	205.2 ± 0.055 ng L^{-1}

4 * smallest increase in the Ag concentration from the addition of highly enriched ^{107}Ag, which is resolvable
5 by measurement of the ^{107}Ag/^{109}Ag isotope ratio using a given technique

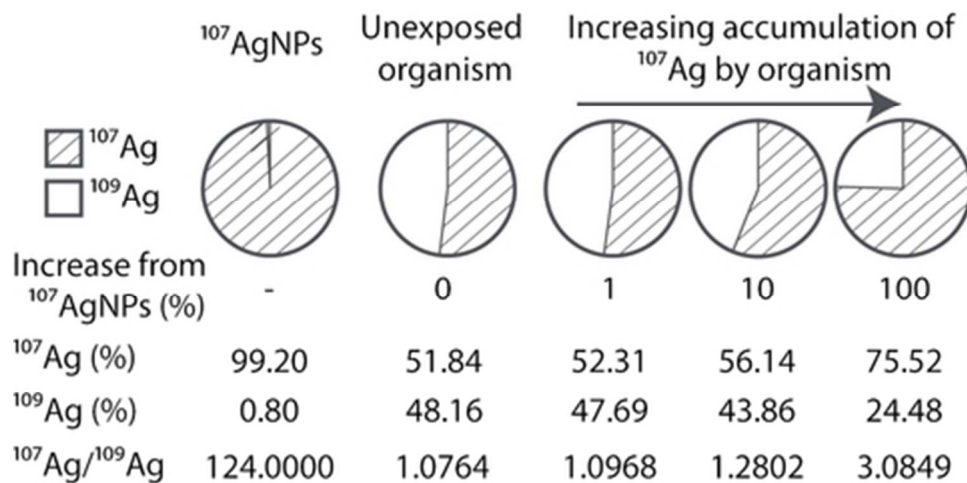|	^{107}AgNPs	Unexposed organism	Increasing accumulation of ^{107}Ag by organism		
Increase from ^{107}AgNPs (%)	-	0	1	10	100
^{107}Ag (%)	99.20	51.84	52.31	56.14	75.52
^{109}Ag (%)	0.80	48.16	47.69	43.86	24.48
^{107}Ag/^{109}Ag	124.0000	1.0764	1.0968	1.2802	3.0849

Fig. 1 Demonstrates how the contribution from isotopically enriched 107Ag to a natural Ag background will result in a deviation in the 107Ag/109Ag that is proportional to the degree of accumulation
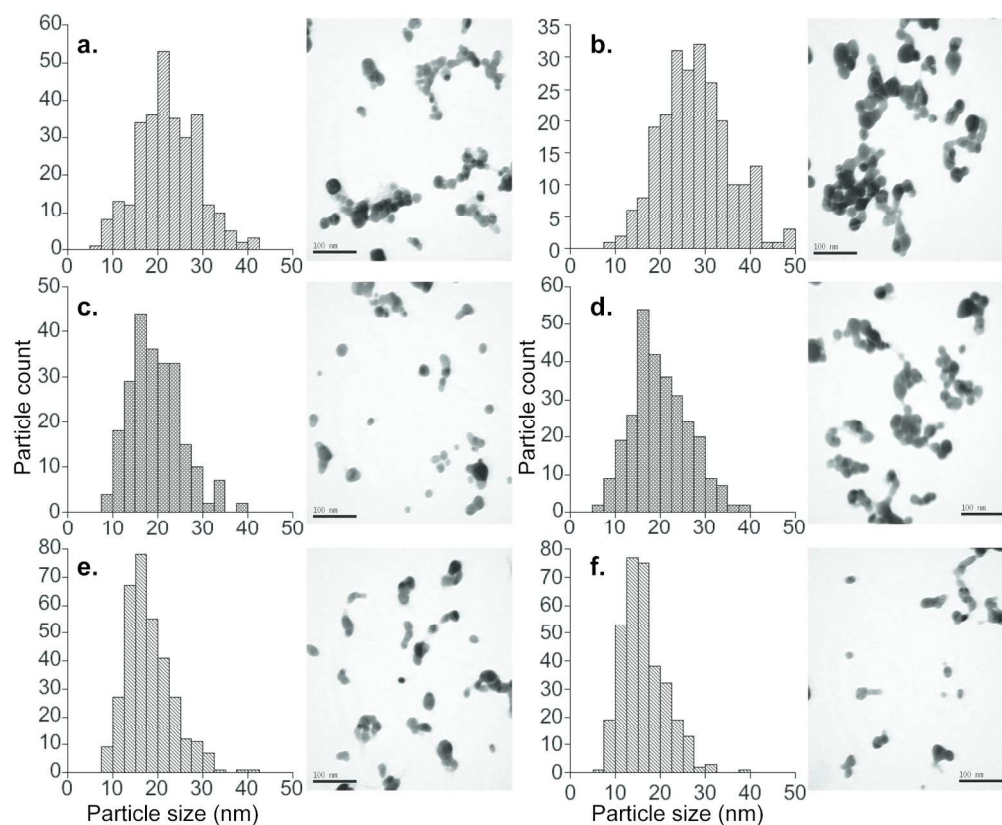40x20mm (300 x 300 DPI)

Fig. 2. TEM images and measured particle size distributions for particles batches synthesised in October 2012. All images are at a magnification of 300,000; scale bars are 0.1µm. (a) Nat-AgNP1-Oct12-F average particle size = 22.3 ± 6.7 nm (1sd) n = 290; (b) 107-AgNP1-Oct12-F average particle size = 28.2 ± 8.3 nm (1sd) n = 236; (c) Nat-AgNP2-Oct12-F average particle size = 19.5 ± 5.7 nm (1sd) n = 234; (d) 107-AgNP2-Oct12-F average particle size = 20.1 ± 6.3 nm (1sd) n = 283; (e) Nat-AgNP3-Oct12-F average particle size = 18.0 ± 5.3 nm (1sd) n = 337; (f) 107-AgNP3-Oct12-F average particle size = 16.3 ± 4.8 nm (1sd) n = 333
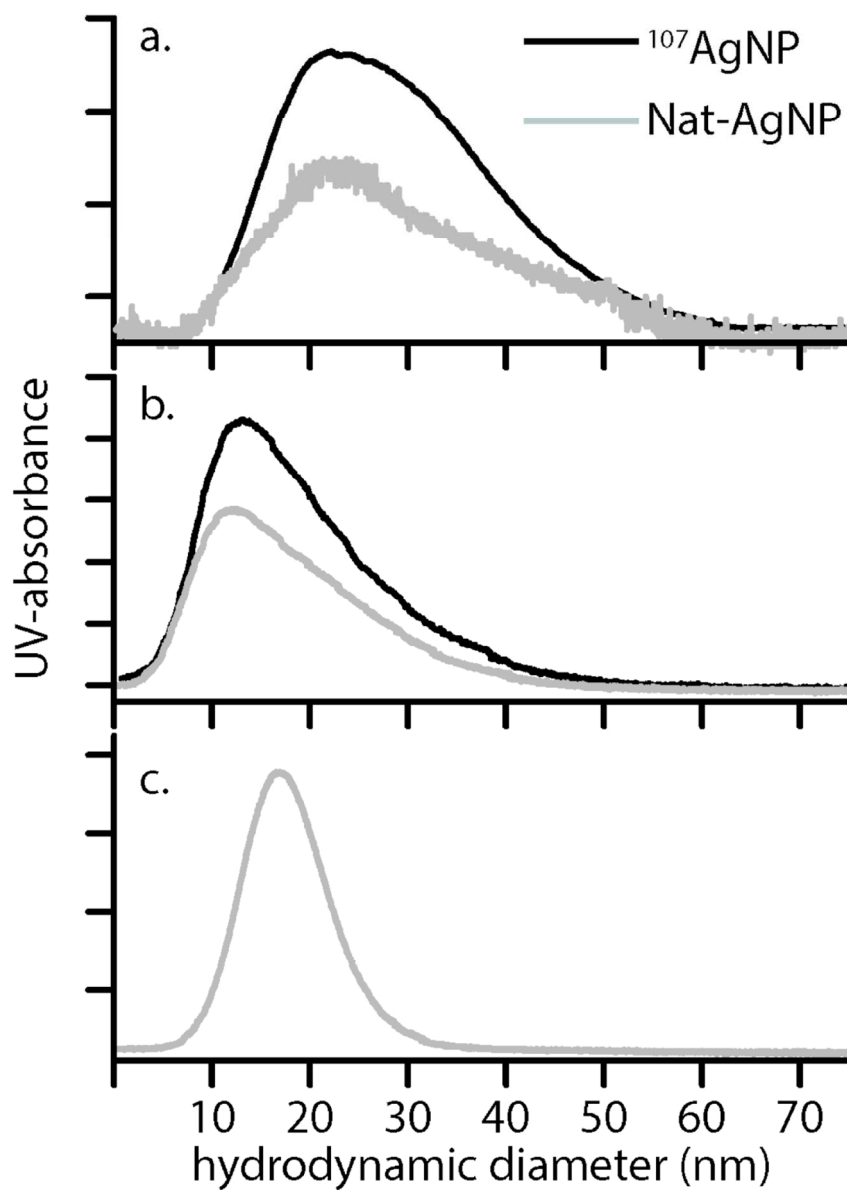
168x137mm (300 x 300 DPI)

Fig. 3: Hydrodynamic diameter distributions determined by FlFFF for selected AgNP batches. (a): 107-AgNP1-May12-F and Nat-AgNP1-May12-F, (b) 107-AgNP2-May12-F, Nat-AgNP2-May12-F and (c) Nat-AgNP3-May12-F
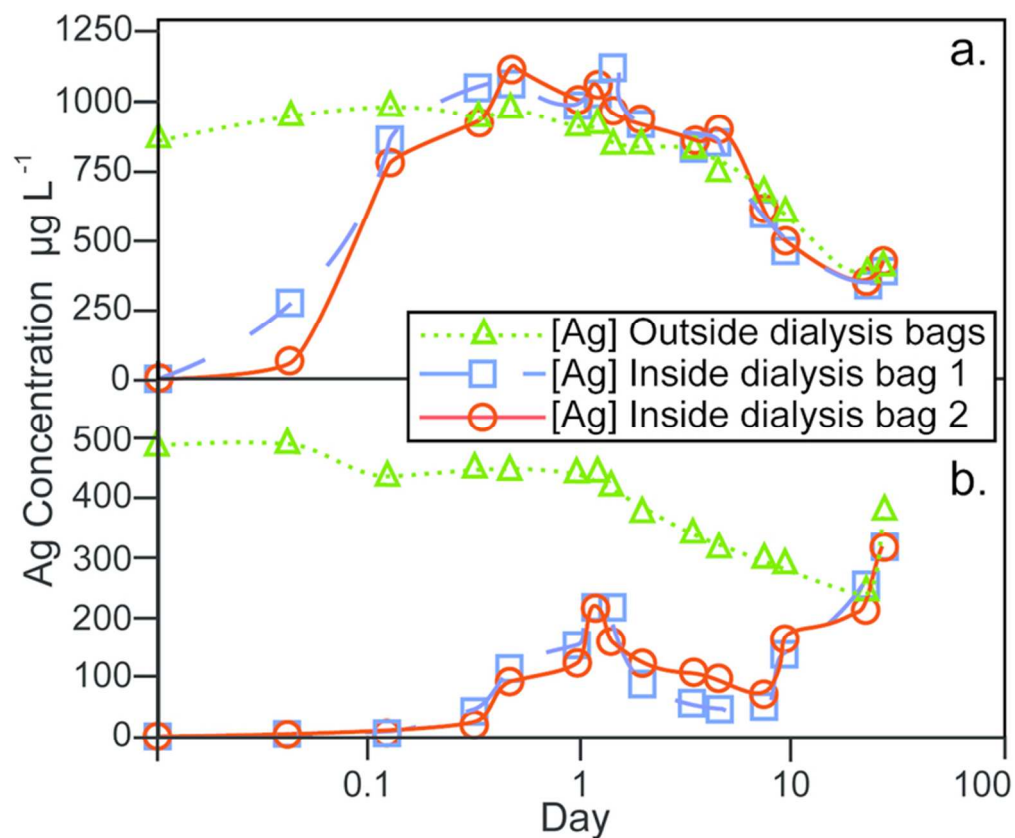115x162mm (300 x 300 DPI)

Fig. 4. Results for AgNP dissolution behavior in dilute-ASW, assessed by dialysis. (a) Control experiment, whereby aqueous AgNO3 solution is added to the dilute ASW outside of the dialysis bags to a concentration of 1 mg L-1. (b) Experiment where 107AgNPs, from particle batch 107-AgNP2-Oct12-F, were added to the dilute-ASW outside of the dialysis bags to a concentration of 0.9 mg L-1
68x56mm (300 x 300 DPI)